Degradation of ibuprofen by photo-based advanced oxidation processes: exploring methods of activation and related reaction routes

Sandyanto Adityosulindro, Carine Julcour-Lebigue, David Riboul, Laurie Barthe

https://doi.org/10.1007/s13762-021-03372-5

Degradation of ibuprofen by photo-based advanced oxidation processes: exploring methods of activation and related reaction routes

S. Adityosulindro[1,2] · C. Julcour[1] · D. Riboul[3] · L. Barthe[1]

Abstract
Several homogeneous photo-based advanced oxidation processes-namely photolysis, photo-oxidation, and photo-Fenton oxidation—were investigated for the elimination of ibuprofen in water. The effects of several operating parameters, such as the lamp type (low or medium pressure mercury, xenon-arc), the concentration of hydrogen peroxide (0.5 to 7 times the stoichiometric amount required for mineralization), and the concentration of Fenton reagent, were quantified. Photo-Fenton oxidation was also combined with low-frequency sonication to investigate possible synergistic interactions. Ibuprofen degradation under ultraviolet photolysis and ultraviolet/hydrogen peroxide oxidation followed pseudo-first-order kinetics with respect to the pollutant concentration and the apparent rate constant increased with lamp power (6–10 W) and oxidant concentration. Photo-Fenton oxidation under ultraviolet light (L1 lamp, 254 nm, 6 W) and visible light (L2 lamp, 360–740 nm, 150 W) led to complete ibuprofen removal after 3 h, but the mineralization yield of the L1/Fenton process (82%) was higher than that of the L2/Fenton process (59%) because of the effects of ultraviolet/hydrogen peroxide oxidation in the former. Coupling L2/Fenton with sonication improved the degradation rate of the molecule at low Fenton reagent concentration, but the beneficial effect of ultrasound on ferrous iron regeneration vanished when the iron to ibuprofen molar ratio was close to 1. An overall reaction scheme for ibuprofen degradation is proposed based on the transformation products detected during these processes.

Keywords Emerging contaminants · Energy demand · Pharmaceuticals · Photo-Fenton · Degradation pathways · Synergy index · Ultrasound activation

Introduction

Clean water is a fundamental human need. Nevertheless, providing sufficient and affordable drinking water to communities worldwide remains a serious challenge. The diversification of industrial and agricultural activities has contributed to the contamination of water resources by anthropogenic compounds. Personal care products, plasticizers, pesticides, contrast media, food additives, wood preservatives, and pharmaceuticals are just a few examples of anthropogenic compounds recognized as emerging contaminants (Petrie et al. 2015; Sophia and Lima 2018).

Interest in pharmaceuticals has recently increased because they are regularly released by a variety of sources, both domestic and industrial, including in agriculture and by livestock (Rehman et al. 2015). Pharmaceuticals are also a particular concern because of their intrinsic biological activity and acute and potentially chronic toxicity (Carlsson et al. 2006; Gadipelly et al. 2014; Lindim et al. 2019). Numerous studies have demonstrated the presence of pharmaceuticals in various environmental matrices around the world, such as wastewater, sludge, rivers, groundwater, soil, and even drinking water (Syakti et al. 2013; Burns et al. 2018; Fekadu et al. 2019; Li et al. 2019; Lindim et al. 2019).

The ubiquitous presence of pharmaceuticals highlights the ineffectiveness of conventional wastewater treatments for these compounds, but also their high stability under sunlight. Conventional biological treatments such as activated

Editorial responsibility: Maryam Shabani.

✉ C. Julcour
carine.julcour@ensiacet.fr

[1] Laboratoire de Génie Chimique, Université de Toulouse, CNRS, INP, UPS, Toulouse, France

[2] Environmental Engineering Study Program, Department of Civil Engineering, Universitas Indonesia, Depok, Indonesia

[3] EcoLab, CNRS, INPT, UPS, Université de Toulouse, Toulouse, France

sludge processes are known to be cost-effective, but antibiotic concentrations as low as 1 mg/L have been reported to have toxic effects on activated sludge bacteria (Välitalo et al. 2017). Previous studies have also found that activated sludge processes only partially remove analgesics, anti-inflammatory drugs, and antibiotics (Deblonde et al. 2011; Tiwari et al. 2017).

Membrane-based separation processes are highly efficient, but they generate pollutant-concentrated streams that then need to be treated in turn (Rosman et al. 2018). In addition, pharmaceuticals are poorly photodegraded under sunlight in water because their maximal spectral absorbance is usually in the ultraviolet range (Packer et al. 2003; Wang and Lin 2014). Whatever the process furthermore, partially degraded pharmaceuticals may be dangerous and intermediates may be even more toxic than the parent compounds (Quero-Pastor et al. 2014).

Another possibility attracting increasing attention in wastewater treatment, especially for the removal of toxic and recalcitrant compounds such as pharmaceuticals, is advanced oxidation. Advanced oxidation processes (AOPs) differ from conventional procedures in that they are based on the generation of reactive oxygen species, chief among them the hydroxyl radical ($^{\bullet}OH$). This powerful and non-selective oxidant degrades organic compounds into innocuous by-products relatively rapidly (within a few minutes) or may even completely mineralize them, with water, carbon dioxide, and inorganic salts as final products. Nevertheless, although the parent compounds are often substantially removed, complete mineralization is in some cases difficult to achieve because of (i) the formation of more recalcitrant by-products (Mrowetz et al. 2003; Jakimska et al. 2014; Quero-Pastor et al. 2014; Li et al. 2015); (ii) the presence of radical scavengers (Tokumura et al. 2016; Adityosulindro et al. 2018); (iii) catalyst deactivation and/or the formation of catalytically inactive complexes (Babuponnusami and Muthukumar 2014; He et al. 2016). Combining several AOPs (creating what are known as hybrid AOPs or HAOPs) is a promising solution to overcome these drawbacks. The basic objective of combining AOPs is to enhance the generation of free radicals, but other synergistic effects have also been reported including (i) the in situ generation of hydrogen peroxide (Torres et al. 2008; Madhavan et al. 2010a; Dükkancı et al. 2014); (ii) the acceleration of a rate-limiting step (Madhavan et al. 2013; Xu et al. 2013; Adityosulindro et al. 2017); and (iii) the destruction of specific compound(s) (Torres et al. 2008; Papoutsakis et al. 2015). In other cases, conversely, combining AOPs has been shown to have only marginal synergistic effects or none at all (Xu et al. 2009; Méndez-Arriaga et al. 2009; Madhavan et al. 2010b, a; Chakma and Moholkar 2014). Numerous binary and ternary combinations of AOPs have been examined in the literature, for example: sono-ozonation, UV-ozonation, and ozone-Fenton, photo-Fenton, sono-Fenton, electro-Fenton, ozone-photo-Fenton, ozone-sono-Fenton, sono-electro-Fenton, and sono-photo-Fenton processes (Bagal and Gogate 2014; Mirzaei et al. 2017; Zhang et al. 2019).

The model contaminant in this study, ibuprofen (IBP), a non-steroidal anti-inflammatory drug (NSAID), was chosen for its toxicity and refractory behavior (Tayo et al. 2018; Parolini 2020). For instance, IBP concentrations of 1–200 mg/L can immobilize *Daphnia Magna* (Du et al. 2016), while its enzyme activity, gene expression, and reproduction can be altered at concentrations as low as 0.5-50 µg/L (Wang et al. 2016). Various AOPs such as ozonation (O_3) (Zwiener 2000), O_3/H_2O_2 (Zwiener 2000), photo-H_2O_2 (Shu et al. 2013), photo-peroxydisulfate (Kwon et al. 2015), TiO_2 photocatalysis (Jallouli et al. 2018), sonolysis (Adityosulindro et al. 2017), Fenton (Adityosulindro et al. 2018), sono-Fenton (Adityosulindro et al. 2017), photo-Fenton (Loaiza-Ambuludi et al. 2014; Tokumura et al. 2016), and sono-photo-Fenton (Méndez-Arriaga et al. 2009; Madhavan et al. 2010c) processes have been applied to remove IBP from water. Although AOPs are difficult to compare, the most effective seems to be the coupling of ozone and hydrogen peroxide treatments, which complete eliminates IBP in 10 min (Zwiener 2000). However, since ozone-based AOPs are expensive (Gonzalez-Olmos et al. 2011), water treatment developments tend rather toward a better use of sunlight (whose spectral power lies mostly in the visible domain, $\lambda = 400$–800 nm) (Gonzalez-Olmos et al. 2012; Funai et al. 2017; Foteinis et al. 2018; Cabrera Reina et al. 2020).

The effects of the power and wavelength of light irradiation were therefore investigated on the effectiveness of photolysis, photo-H_2O_2, and photo-Fenton processes for the removal of IBP. A possible enhancement of the photo-Fenton reaction by low-frequency ultrasound was also evaluated, as were the reaction intermediates formed during the different oxidative treatments.

Materials and methods

Chemicals and solvents

Ibuprofen ($C_{13}H_{18}O_2$; purity 99.99%) was purchased from BASF Corporation and used as received. Hydrogen peroxide (30% w/w H_2O_2 in water), sulfuric acid (1 M H_2SO_4), monopotassium phosphate (KH_2PO_4), sodium phosphate dibasic dehydrate ($Na_2HPO_4{\cdot}2H_2O$), potassium iodide (KI), titanium tetrachloride (0.09 M $TiCl_4$ in 20% HCl), sodium sulfite (Na_2SO_3) and iron sulfate heptahydrate ($FeSO_4{\cdot}7H_2O$) were obtained from Sigma-Aldrich.

Experimental setup

Experiments were performed in a batch reactor assembly consisting of a photochemical reactor (0.5 L capacity) and a sono-reactor (1 L capacity), unless otherwise specified. Ibuprofen solution was circulated between the two using a peristaltic pump (with a flow rate of 150 mL/min). The reactors were connected to a thermostatic bath to maintain a constant temperature (25 °C). The degradation of ibuprofen was evaluated under four different light sources placed in a quartz immersion well: two low pressure mercury lamps (L1 and L1′), a xenon-arc lamp (L2), and a medium pressure mercury lamp (L3). The interesting features of L1 (a 6 W LP Hg lamp) are its low capital and operating costs, while the emission spectrum of L2 (a 150 W xenon-arc lamp) mimics sunlight. The sono-reactor was a cup-horn sonicator, equipped with an impeller, a temperature probe, and sampling tubes (Fig. S1 in supplementary information). The characteristics of the lamps and the ultrasound device are given in Table S1 (in supplementary information).

Experimental procedure

AOPs are known to be well-suited for the treatment of wastewaters containing recalcitrant and toxic contaminants at low to moderate concentrations, typically from less than 5 ppb to several hundred ppm, avoiding the consumption of large amounts of expensive reagents (Andreozzi 1999; Munter 2001). Nonetheless, they are usually more economically viable in the upper loading range, because the oxidant is used more efficiently (Miralles-Cuevas et al. 2013). In this study, therefore, a synthetic solution with 20 mg/L or 0.1 mM IBP (equivalent to about 15 mg/L of total organic carbon) was prepared by dissolving 40 mg of ibuprofen powder in 2 L of distillated water. The solution was stirred for 14 h at 25 °C using a magnetic stirrer (600 rpm) to ensure complete dissolution of the IBP. The resulting pH was 4.3.

The solution (1.5 L) was poured and circulated between the reactors for about 5 min, before a first sample was withdrawn once the desired temperature had been reached (defining the start of the reaction, $t = 0$). The lamp was then turned on for 2 min before adding H_2O_2 to achieve constant irradiation prior to oxidation. For the Fenton reactions, the IBP solution was mixed with iron salt ($FeSO_4.7H_2O$) and the pH was adjusted to 2.6 with a 1 M solution of H_2SO_4 before being circulated.

Aliquots were withdrawn throughout the reaction (at $t = 5$, 10, 30, 60, 120, and 180 min). Before chromatography analysis of the Fenton-treated samples, 1 mL of the sample was immediately treated with 1 mL of phosphate solution (a mixture of 0.05 M KH_2PO_4 and 0.05 M $Na_2HPO_4.2H_2O$), then passed through a 0.45 µm RC syringe filter to remove the resulting iron precipitate and stop the reaction. In addition, before total organic carbon (TOC) measurements, 8 mL of the sample was treated with 3 mL of a quenching solution (a mixture of phosphate buffer, 0.1 M KI and 0.1 M Na_2SO_3 to reduce residual H_2O_2), filtered (using a 0.45 µm RC syringe filter) and diluted twofold with ultrapure water.

Analytical techniques

The evolution of the ibuprofen concentration during the experiments was monitored by high-performance liquid chromatography (HPLC) with UV detection at $\lambda = 222$ nm (PDA detector, Thermo Finnigan). Separation was carried out on a C18 reverse phase column (ProntoSIL C18 AQ 5 µm, 250 × 4 mm) at 40 °C. The mixture of acetonitrile and acidified water (with 0.1% v/v phosphoric acid) was fed in isocratic mode (60/40) at 1 mL/min.

Total organic carbon (TOC) concentrations were calculated based on total carbon (TC) and inorganic carbon (IC) measurements performed using a TOC analyzer (TOC–L, Shimadzu Corp.). The injection volumes for the TC and IC measurements were 50 µL and 400 µL, respectively.

Residual concentrations of hydrogen peroxide at the end of each experiment were measured using the titanium tetrachloride method (O'Sullivan and Tyree 2007). Samples (5 mL) were diluted to 25 mL, then mixed with 1 mL of $TiCl_4$ solution and 1 mL of H_2SO_4 solution (1 M). The formation of pertitanic acid (yellow color) was detected using a spectrophotometer at 410 nm.

The transformation products during the reaction were identified by high-performance liquid chromatography–high-resolution mass spectrometry (HPLC–HRMS). These analyses were carried out using an ACCELA LC system coupled to an Exactive™ Orbitrap Mass Spectrometer (Thermo Fisher Scientific, San Jose, the USA). Separation was performed using a PFP column (Phenomenex Luna PFP2, 150 mm × 2 mm, 3 µm) at 40 °C. The mobile phases, (A) ultrapure water acidified with 0.1% v/v formic acid and (B) acetonitrile, were eluted in gradient mode: 3% B for 5 min, 3 to 95% B over the following 20 min, 95% B for $t = 25$–30 min, 95 to 3% B within 1 min and 3% B for $t = 31$–37 min. The injection volume and flow rate were 5 µL and 0.2 mL/min, respectively. The HRMS analysis was performed with electrospray ionization (ESI) in both positive and negative ion modes. The source parameters were as follows: sheath gas flow rate and auxiliary gas flow rate = 50 and 20 arbitrary units, respectively; capillary temperature = 350 °C; spray voltage = + 3 kV (positive polarity) and − 3 kV (negative polarity). The m/z scan range was 50 to 1000, and the resolution was set to 100,000 full width at half maximum (FWHM) at 1 Hz. The automatic gain control (AGC) target was set to a high dynamic range (3×10^6), and the maximum injection time was 100 ms. The instrument was calibrated every 24 h using the manufacturer's

calibration protocol. The formulas of the intermediate products were predicted based on the exact mass of the monoisotopic peak and the relative abundances of the isotope peaks using the software programs Xcalibur (version 2.0, Thermo scientific Inc.) and MetAlign (version 041011, Arjen Lommen).

Results and discussion

Photolysis

The degradation mechanism of IBP was first evaluated under ultraviolet (UV) photolysis.

Ibuprofen can be degraded by UV light through several mechanisms:

(i) direct photo-degradation, producing excited IBP (IBP*), which then undergoes bond cleavage (Eqs. 1–2) (Oppenländer 2003; Li et al. 2015);
(ii) photosensitization, in which IBP* transfers its energy to dissolved oxygen, generating a high energy form of oxygen (singlet molecular oxygen ($^1O_2$)), which subsequently attacks IBP (Eqs. 3–4) (Oppenländer 2003; Li et al. 2015) or produces active radicals (Eqs. 5–8) (Parsons 2004; Na et al. 2012);
(iii) UV-driven homolysis of water, which produces $^{\bullet}OH$ radicals that then react with the IBP (Gonzalez et al. 2004; Son et al. 2009; da Silva et al. 2014).

The latter mechanism can be excluded given the emission spectrum of the lamps, as water photolysis occurs only with wavelengths shorter than 200 nm.

$$IBP + h\nu_{(\lambda=200-280)} \rightarrow (IBP)^* \quad (1)$$

$$(IBP)^* \rightarrow \text{Degradation products} \quad (2)$$

$$(IBP)^* + {}^3O_2 \rightarrow IBP + {}^1O_2 \quad (3)$$

$$(IBP) + {}^1O_2 \rightarrow \text{Degradation products} \quad (4)$$

$$(IBP)^* + O_2 \rightarrow (IBP)^{\bullet+} + O_2^{\bullet-} \quad (5)$$

$$2O_2^{\bullet-} + 2H^+ \rightarrow H_2O_2 + O_2 \quad (6)$$

$$H_2O_2 + h\nu_{(\lambda=185-300\ nm)} \rightarrow 2\ ^{\bullet}OH \quad (7)$$

$$^{\bullet}OH/O_2^{\bullet-} + IBP \rightarrow \text{Degradation products} \quad (8)$$

To separate the contributions of direct photo-degradation, radical attack and singlet molecular oxygen, preliminary photolysis experiments were conducted as follows: (i) without a scavenger, (ii) with methanol as a radical scavenger, and (iii) with nitrogen gas bubbling to prevent the formation of radicals or singlet molecular oxygen. Since methanol transmits more than 95% of radiation with wavelengths longer than 250 nm, it can safely be assumed that adding it had no effect on IBP photon absorption during photolysis and did not quench the effects of $^1O_2$ (Li et al. 2015). These experiments were carried out in the photochemical reactor (0.5 L) irradiated by lamp L1 for 180 min. The IBP removal yield was lower (47% versus 69%) in the presence of 50 mM methanol, and likewise around 50% under anoxic conditions. These results indicate that the main degradation mechanism of IBP under UV light irradiation is direct photolysis (Eq. 1–2), with a smaller contribution from radical attack (Eq. 5–8), while the effect of singlet molecular oxygen seems to be negligible.

In addition, Fig. 1 shows that while substantial photolysis of IBP occurred under ultraviolet light (L1, L1′, and L3), the pollutant concentration remained stable under visible light irradiation (L2). The degradation of IBP under UV light can be attributed to its high spectral absorption in the UV-C

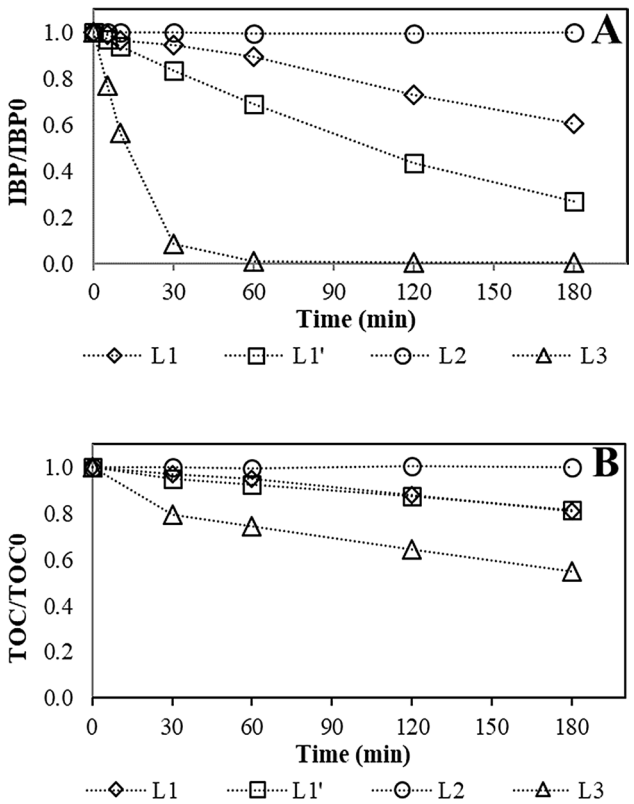

Fig. 1 Effect of lamp type on the photo-degradation of IBP: evolution of **a** IBP and **b** TOC concentration ($[IBP]_0 = 20$ mg/L, $pH_0 = 4.3$, $T = 25$ °C, irradiated volume = 500 mL, total volume = 1500 mL)

region ($\lambda = 200$–280 nm). An improvement in IBP degradation at 254 nm (40% *vs.* 73% of the initial concentration after 180 min) was observed when the power of the lamp was increased from 6 to 10 W. With lamp L3 (a 150 W MP Hg lamp), the reaction was much faster, with complete conversion occurring in just 1 h ($k = 0.0567$ min^{-1}, $R^2 = 0.9969$; Fig. 1a). This result is in agreement with those of Shu and coworkers (Shu et al. 2013), who found that IBP was efficiently degraded ($k = 0.0970$ min^{-1}, $R^2 = 0.9980$) under MP Hg lamp (1000 W/60 mL volume). The better performance of the MP Hg lamp can be ascribed to both its higher power and larger emission band in the UV-C region (up to 21% of the spectral power). Conversely, as expected from its absorption spectrum, IBP was negligibly degraded under visible light (L2, 360–740 nm). This result also indicates that the photo-degradation of IBP under sunlight in the natural environment is likely to be very limited.

In terms of mineralization efficiency, TOC removal was 45% after 3 h of irradiation with L3 versus 19% with L1 (Fig. 1b). Note that in the latter case, increasing the lamp power to 10 W had only a marginal effect, probably because the photoactive intermediates formed were less photoactive (Szabó et al. 2011; da Silva et al. 2014).

Photo-H_2O_2 process

Hydrogen peroxide (H_2O_2) is known to be an effective promoter of photo-initiated oxidation reactions (Klavarioti et al. 2009; Wols and Hofman-Caris 2012). The O–O bond can be cleaved under UV irradiation, producing highly reactive hydroxyl radicals (Eq. (7)) (Oppenländer 2003; Babuponnusami and Muthukumar 2014). The effect of H_2O_2 addition was first studied with L1. As expected, IBP removal was better with H_2O_2 than when light irradiation was used alone (Fig. 2a). For instance, adding 6.4 mM H_2O_2 led to an increase in the apparent first-order rate constant for IBP degradation under L1 from 0.0028 min^{-1} to 0.0664 min^{-1} (i.e., a 24-fold increase).

Figure 2a shows the results of a set of experiments in which the H_2O_2 concentration was varied between 1.6 and 22.4 mM (corresponding to 0.5 to 7 times the stoichiometric amount required for complete mineralization). The IBP oxidation rate increased with the H_2O_2 concentration up to 6.4 mM before leveling off, indicating that $^{\bullet}OH$ scavenging occurs at high H_2O_2 excess (Eq. 9) (Cruz González et al. 2018; Adak et al. 2019).

$$H_2O_2 + {}^{\bullet}OH \rightarrow {}^{\bullet}OOH + H_2O \quad (9)$$

The optimum concentration of H_2O_2 for TOC conversion was similarly found to be 6.4 mM (Fig. 2b). However, measurements of residual H_2O_2 concentrations showed

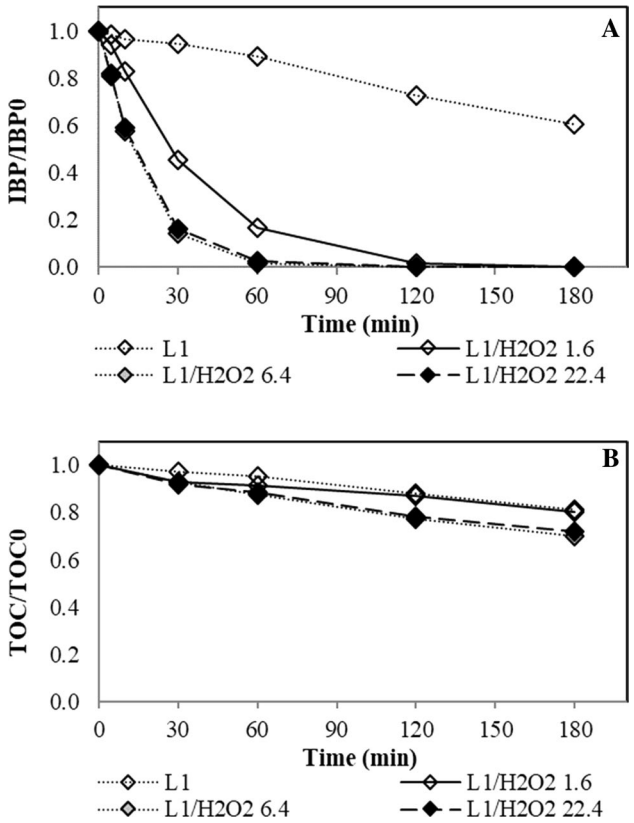

Fig. 2 Effect of H_2O_2 dose on the photo-assisted degradation of IBP: **a** IBP and **b** TOC concentration: ($[IBP]_0 = 20$ mg/L, $pH_0 = 4.3$, $T = 25$ °C, irradiated volume = 500 mL, total volume = 1500 mL, $[H_2O_2]_0 = 0$–22.4 mM)

that the LP Hg lamp only partially converted the oxidant (with decomposition rates ranging from 13% at 1.6 mM H_2O_2 to 15% at 22.4 mM H_2O_2) within 3 h.

The effect of H_2O_2 addition (6.4 mM) was also assessed for the three other lamps. This led to a fivefold increase in the apparent degradation rate constant with L3 (from 0.0567 to 0.2610 min^{-1}; Fig. 3a). However, since the photolysis of IBP with L3 was already very effective, the relative contribution of H_2O_2 decomposition was less than observed for L1 and L1′. Weak IBP degradation was also observed under L2/H_2O_2, which was not expected given the negligible absorbance of IBP and H_2O_2 in the visible light region.

In terms of TOC removal, photo-H_2O_2 oxidation with the MP Hg lamp led to almost complete mineralization (97%) after 3 h, compared with mineralization yields of just 30%, 46%, and 5% with L1, L1′, and L2, respectively (Fig. 3b). Analysis of the residual H_2O_2 showed that almost all the oxidant was consumed with L3, which thus induced rapid photolysis of IBP and effective photodecomposition of H_2O_2, enabling high TOC removal.

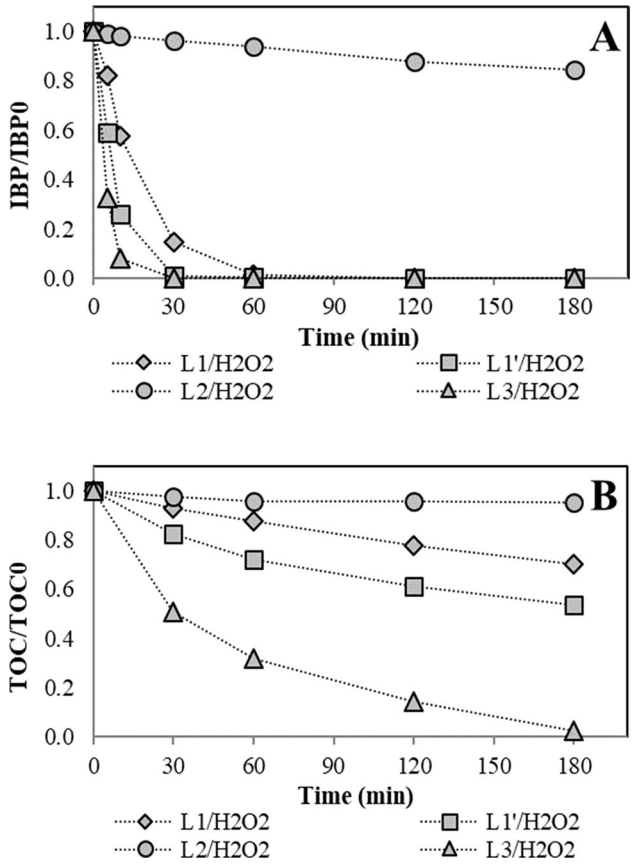

Fig. 3 Effect of lamp type on the photo-oxidation of IBP: **a** IBP and **b** TOC concentration: ($[IBP]_0$ = 20 mg/L, pH_0 = 4.3, T = 25 °C, irradiated volume = 500 mL, total volume = 1500 mL, $[H_2O_2]_0$ = 6.4 mM)

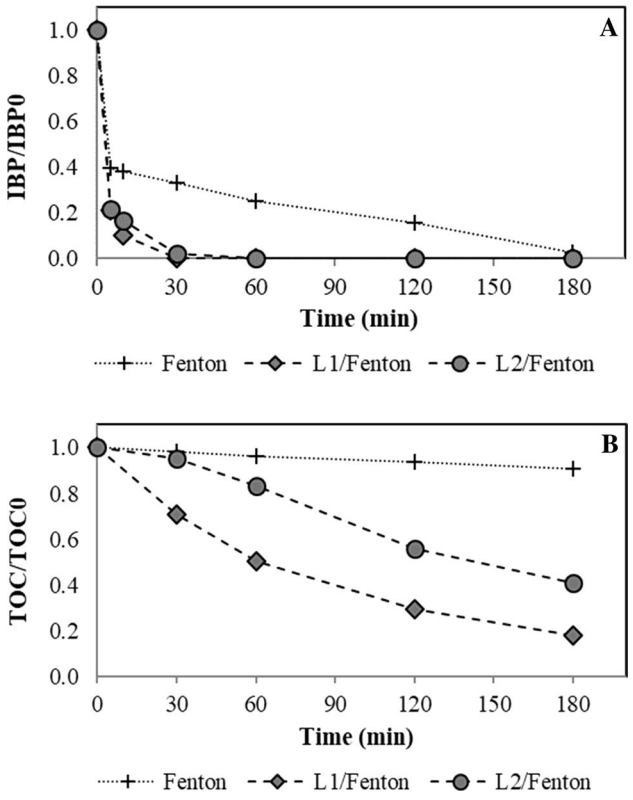

Fig. 4 Effect of lamp type on the photo-Fenton oxidation of IBP: **a** IBP and **b** TOC concentration: ($[IBP]_0$ = 20 mg/L, pH_0 = 2.6, T = 25 °C, irradiated volume = 500 mL, total volume = 1500 mL, $[H_2O_2]_0$ = 6.4 mM, [Fe] = 0.134 mM)

Photo-Fenton process

Photo-Fenton oxidation experiments were conducted using L1 and L2. Fenton reagent was prepared with 6.4 mM H_2O_2 and 0.134 mM Fe^{2+} (i.e., Fe:H_2O_2 = 1:48 mol/mol). A Fenton experiment was also carried out without light irradiation for comparison.

Figure 4 shows that the IBP and TOC oxidation rates in the photo-Fenton experiments were much higher than observed with the other processes, highlighting the expected synergistic interaction. The L2 lamp was also found to be very efficient in the photo-Fenton process, although it did not outperform L1. Both lamps enabled much higher H_2O_2 consumption (80% for L2 and 99% for L1) than when Fenton oxidation was used alone (13%).

Given that L1's nominal power is much lower than L2's, the remarkable mineralization efficiency with the former can be attributed to the additional $^{\bullet}OH$ groups formed by H_2O_2 photolysis (Eq. 7), but also to the photo-reduction of ferric ions and of H_2O_2-iron(III) complexes (Eqs. 10–12), whose yields are higher with UV-C rather than UV-A or visible irradiation (Safarzadeh-Amiri et al. 1997; Pérez 2002). On the other hands, the irradiation from L2 probably enhanced the photo-decarboxylation of the complexes formed by ferric ions with the short-chain organic acids produced during the reaction (Eq. 13) (Waite and Morel 1984; Safarzadeh-Amiri et al. 1997; Rodríguez et al. 2009; Nichela et al. 2015).

$$Fe^{3+} + H_2O + hv_{(\lambda<300\ nm, \lambda\ max=240\ nm)} \rightarrow Fe^{2+} + {}^{\bullet}OH + H^{+} (pH < 4) \quad (10)$$

$$Fe(OH)^{2+} + hv_{(\lambda=200-400\ nm,\ \lambda\ max=205;297\ nm)} \rightarrow Fe^{2+} + {}^{\bullet}OH (pH = 2-4) \quad (11)$$

$$Fe - OOH^{2+} + hv_{(\lambda=180-550\ nm)} \rightarrow Fe^{2+} + {}^{\bullet}OOH \quad (12)$$

$$\left[Fe^{III}(RCO_2)\right]^{2+} + hv_{(\lambda=365-600\ nm)} \rightarrow Fe^{2+} + RCOO^{\bullet} \quad (13)$$

Sono-photo-Fenton processes

Low-frequency sonication (at 20 kHz) is known to be effective for the sono-oxidation of IBP (Adityosulindro et al. 2017).

The effects of sonication on the photo-Fenton oxidation of IBP were evaluated for the previous concentration of Fenton reagent (0.134 mM Fe^{2+}, 6.4 mM H_2O_2) and a lower one (0.033 mM Fe^{2+}, 1.6 mM H_2O_2) with the same Fe/oxidant molar ratio (Fe:H_2O_2 = 1:48). The lower concentration was investigated to minimize the post-reaction iron concentration and highlight possible interactions between ultrasound and light irradiation.

In Fig. 5a, the effects of the ultrasound treatment are clearer at the lower reagent concentration. With this combined process, IBP was fully converted after 180 min of oxidation, while the conversion rate with the photo-Fenton (L2/Fenton(-)) process was 76%.

To highlight the benefits of combining AOPs, a synergy factor (SF) was calculated using Eq. (14), as proposed by various authors (Weavers et al. 1998; Dükkancı et al. 2014):

$$\mathrm{SF} = \frac{k_{\text{Combined process}}}{\left(k_{\text{process 1}} + k_{\text{process 2}} + k_{\text{process } i} + \ldots + k_{\text{process } n}\right)} \quad (14)$$

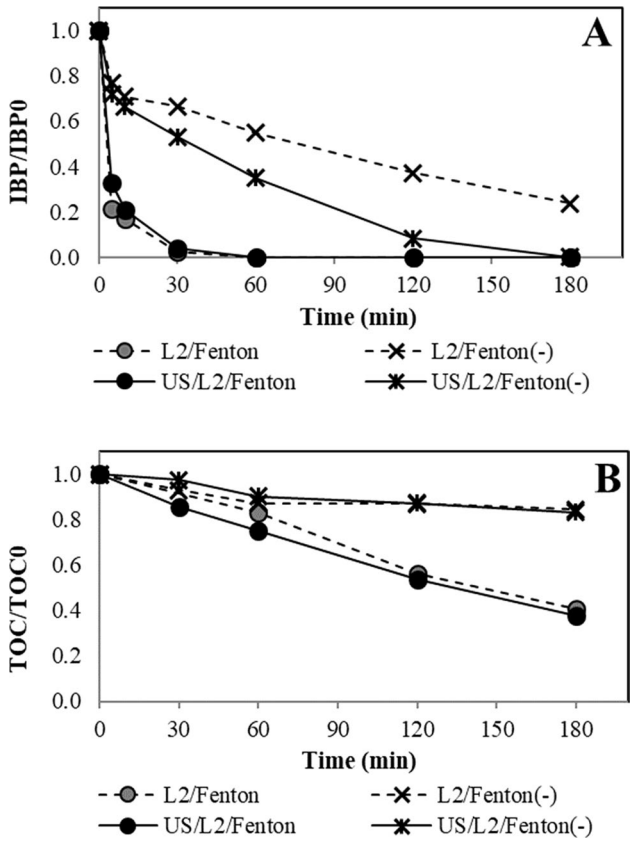

Fig. 5 Comparison of photo-Fenton and sono-photo-Fenton oxidations of IBP: **a** IBP and **b** TOC concentration: ($[IBP]_0$ = 20 mg/L, pH_0 = 2.6, T = 25 °C, irradiated volume = 500 mL, sonicated volume = 1000 mL, total volume = 1500 mL, f_{US} = 20 kHz, D_{US} = 50 W/L, $[H_2O_2]_0$ = 1.6–6.4 mM, [Fe] = 0.033–0.134 mM, low concentration of Fenton reagent denoted as (−))

where k refers to the apparent first-order rate constant for pollutant degradation.

The hybrid process can thus be considered synergistic if SF > 1.

Since the degradation of IBP by Fenton-related processes was very rapid in the first 5 min, the apparent reaction rate constants were calculated from that time onward (see Tables 1 and 2). The synergistic effect of combining the Fenton process with visible light (SF = 8.1) was much higher than when it was combined with ultrasound (SF = 2.0). The superior activation performance of visible light over ultrasound can be ascribed to its higher efficiency in ferrous iron regeneration. Nonetheless, at the low Fenton reagent concentration (Fe/IBP molar ratio of ~ 0.3), the competition for photons between ferric ions/complexes and IBP (and its intermediates) may impede the photo-reduction of the former. This phenomenon has already been reported elsewhere and is referred to as the "inner filter effect" (Andreozzi 1999; Xu et al. 2013).

Thus, while the rate constant for the ternary process (US/L2/Fenton) was higher than the sum of the k values for each process separately (US, L2, Fenton), this is actually due to an additive effect of the two activated Fenton processes (US/Fenton + L2/Fenton).

Table 1 First-order degradation rate constant of IBP for the separate and combined processes

Process	k^a (min^{-1})	R^2
US[b]	0.0035	0.9787
L2	Negligible	N/A
Fenton[c]	0.0008	0.9940
US/Fenton[c]	0.0088	0.9940
L2/Fenton[c]	0.0065	0.9955
US/L2/Fenton[c]	0.0130	0.9975

[a]Based on IBP concentration–time profile after 5 min of reaction

[b]Cited from a previous study (Adityosulindro et al. (2017))

[c]Low concentration of Fenton reagent ($[H_2O_2]_0$ = 1.6 mM, [Fe] = 0.033 mM)

Table 2 Synergy factor (SF) of the combined processes (based on the apparent first-order rate constants of (Table 1)

Process	Equation	SF
US/Fenton	$k_{\text{US/Fenton}}/(k_{\text{US}} + k_{\text{Fenton}})$	2.0
L2/Fenton	$k_{\text{L2/Fenton}}/(k_{\text{L2}} + k_{\text{Fenton}})$	8.1
US/L2/Fenton	$k_{\text{US/L2/Fenton}}/(k_{\text{US}} + k_{\text{L2}} + k_{\text{Fenton}})$	3.0
	$k_{\text{US/L2/Fenton}}/(k_{\text{US/Fenton}} + k_{\text{L2}})$	1.5
	$k_{\text{US/L2/Fenton}}/(k_{\text{US}} + k_{\text{L2/Fenton}})$	1.3
	$k_{\text{US/L2/Fenton}}/(k_{\text{US/Fenton}} + k_{\text{L2/Fenton}})$	0.9

For TOC removal on the other hands, combining the three processes had little benefit, with 17% TOC removal with the sono-photo-Fenton process versus 15% with the photo-Fenton process (Fig. 5b). At the reference reagent concentration moreover (0.134 mM Fe^{2+}, 6.4 mM H_2O_2), the performances of the sono-photo-Fenton and photo-Fenton processes were similar in terms of both IBP and TOC removal.

Evaluation of electric energy and oxidant consumption

Despite their recognized efficiency, UV/H_2O_2-based processes are rarely implemented on an industrial scale because of the potentially high operating costs associated with inefficient oxidant use and the lamp's energy consumption.

The energy costs of AOPs can be compared using the electrical energy per order (EEO). The EEO is the electrical energy per unit volume required to degrade a contaminant C by one order of magnitude (Eq. 15) (Bolton et al. 2001), and thus, a smaller value indicates lower energy consumption:

$$\mathrm{EEO} = \frac{(P \times t \times 1000)}{\left(V \times 60 \times \log\left(\frac{C_i}{C_t}\right)\right)} \quad (15)$$

where EEO is the electrical energy per order of pollutant removal (kWh/m^3/order), P is the power input (kW), t is the reaction time (min), V is the volume of solution in the reactor (L), C_i is the initial pollutant concentration (20 mg/L), and C_t is concentration of pollutant at reaction time t.

Furthermore, the amounts of H_2O_2 consumed for pollutant mineralization can be compared using the oxidant consumption index (OCI) (Shahbazi et al. 2014). A smaller OCI indicates lower oxidant consumption (thus higher oxidant efficiency) as shown in the following equation:

$$\mathrm{OCI} = \frac{\Delta[H_2O_2]}{\Delta[\mathrm{TOC}]} \quad (16)$$

where $\Delta[H_2O_2]$ and Δ[TOC] are the amount of H_2O_2 consumed (mg/L) and TOC removed (mg/L) during 180 min reaction, respectively.

The EEO and OCI values calculated for the different processes are presented in Table 3 and compared to the ones from previous works.

The most energy efficient UV lamp for photolysis was L1′. With L1 and L1′, the addition of H_2O_2 significantly reduced the energy required for pollutant abatement. Note that the EEO values calculated for the photo-H_2O_2 process using the LP Hg lamp (1.9–2.4 kWh/m^3/order)

Table 3 Electric energy and oxidant consumption of the tested processes

Processes	k_{IBP} (min^{-1})	EEO_{IBP} (kWh/m^3/order)	$\Delta[H_2O_2]$ (mg/L)	Δ[TOC] (mg/L)	OCI (mg-H_2O_2/mg-TOC)
L1	0.0028	54.1	0	2.9	0
L1′	0.0074	35.2	0	2.9	0
L2	N/A[d]	N/A	0	0.0	N/A
L3	0.0567	66.9	0	6.8	0
L1/H_2O_2[a]	0.0664	2.4	30.5	4.5	6.7
L1′/H_2O_2[a]	0.1352	1.9	106.6	6.0	17.6
L2/H_2O_2[a]	N/A[d]	N/A	10.9	0.8	14.4
L3/H_2O_2[a]	0.261	15.2	215.4	14.7	14.7
L1/Fenton[b]	Initially fast	N/A	215.4	12.4	17.4
L2/Fenton[b]	Initially fast	N/A	174.1	8.9	19.5
L2/Fenton[c]	Initially fast	N/A	8.2	2.3	3.6
US/L2/Fenton[b]	Initially fast	N/A	165.4	9.4	17.6
US/L2/Fenton[c]	Initially fast	N/A	13.6	2.6	5.3
UV/H_2O_2[e]	N/A	0.09–1.5	N/A	N/A	N/A
Photo/Fenton[e]	N/A	0.07–2.0	N/A	N/A	N/A
Photo/Fenton[f]	N/A	N/A	140	35.6	3.9

[a] $[H_2O_2]_0 = 6.4$ mM

[b] $[H_2O_2]_0 = 6.4$ mM and [Fe] = 0.134 mM

[c] Low concentration of Fenton reagent: $[H_2O_2]_0 = 1.6$ mM and [Fe] = 0.033 mM

[d] Negligible IBP removal

[e] Miklos et al. (2018)

[f] Velichkova et al. (2016)

are comparable to the ones reported in previous studies (0.07–2.0 kWh/m^3/order) and compiled by Miklos and coworkers (Miklos et al. 2018). However, while H_2O_2 decomposition was more efficient under L1′ than under L1, this was not associated with improved TOC removal, and the OCIs of the L1′ and L3 lamps are similar (the energy consumption of the latter being much higher, however, with a much higher contribution from photolysis).

The Fenton-based processes could not be assessed in terms of EEO as the degradation rate was too fast in the initial stages of the reaction. Their OCI was lower at the lower reagent concentration, suggesting that adding Fenton reagent in excess is not worthwhile. This interpretation is not straightforward, however, since the mineralization yields achieved in the two experiments differed and the relative importance of the competitive reactions consuming the oxidant possibly changed in the course of the degradation process (depending on the reactivity of the reaction intermediates).

Overall degradation pathway

Oxidation intermediates were monitored during (i) photolysis under L1, (ii) photo-H_2O_2 oxidation with L1 (L1/H_2O_2), and (iii) photo-Fenton oxidation with L2 (L2/Fenton). Results of the latter experiment were compared with those from a dark Fenton process. Samples collected at various time intervals during the corresponding experiments were analyzed by HPLC-HRMS, and product identifications were verified using standards when available.

Up to 15 transformation products (TPs) were detected during the selected photo-based processes (Table 4). According to the literature, the principal reactions involved in IBP degradation by AOPs are hydroxylation, decarboxylation, and cleavage of the C-C bond.

The free-radical initiated degradation pathway starts with electrophilic attack by $^{\bullet}OH$ of the aromatic ring or the side chains of the molecule (the methylpropyl moiety or the phenylpropionic moiety), forming various hydroxylated IBP compounds, four of which having been found here (TP1A-D). These hydroxylated compounds can be

Table 4 Detected compounds from HPLC-HRMS during selected photo-based AOPs

Code	Elemental composition	t_R (min)	Ion	m/z	L1	L1/H_2O_2	L2/F	F
TP1A	$C_{13}H_{18}O_3$ 1-hydroxy-IBP[a]	19.75	$[M-H]^-$	221.1183	ND	D	D	ND
TP1B[b]	$C_{13}H_{18}O_3$ 2-hydroxy-IBP[a]	18.70	$[M-H]^-$	221.1183	ND	D	D	ND
TP1C[b]	$C_{13}H_{18}O_3$	21.15	$[M-H]^-$	221.1183	D	D	D	D
TP1D[b]	$C_{13}H_{18}O_3$	22.15	$[M-H]^-$	221.1183	D	D	D	D
TP2A	$C_{13}H_{18}O_4$	19.8	$[M-H]^-$	237.1132	ND	D	D	D
TP2B[c]	$C_{13}H_{18}O_4$	20.50	$[M-H]^-$	237.1132	D	D	D	D
TP3A	$C_{13}H_{18}O_5$	18.35	$[M-H]^-$	253.1081	ND	D	D	D
TP3B[d]	$C_{13}H_{18}O_5$	18.65	$[M-H]^-$	253.1081	ND	D	D	D
TP3C[d]	$C_{13}H_{18}O_5$	19.15	$[M-H]^-$	253.1081	ND	D	D	D
TP4	$C_{12}H_{16}O$ 4-isobutylacetophenone[a]	25.1	$[M+H]^+$	177.1273	D	ND	ND	ND
TP5[e]	$C_{12}H_{16}O$	20.95	$[M-H]^-$	175.1128	D	D	D	D
TP6	$C_9H_8O_3$	16.75	$[M-H]^-$	163.0400	D	D	D	D
TP7	$C_9H_{10}O_2$ 2-phenyl-propionic acid	16.8	$[M-H]^-$	149.0608	D	D	D	D
TP8	$C_9H_{10}O$	17.7	$[M-H]^-$	133.0658	D	D	D	D
TP9	$C_5H_{10}O_3$	~4.0	$[M-H]^-$	117.0557	D	D	D	D

A minimum peak intensity of 1000 and a maximum mass deviation of 10 ppm were considered for detection threshold and molecule identification, respectively. "Elemental composition" refers to the unionized molecule, "ion" refers to the elemental composition of the detected ion possessing an exact mass of "*m/z*"

[a]Confirmed by standard

[b]Isomer of TP1A

[c]Isomer of TP2A

[d]Isomer of TP3A

[e]Isomer of TP4

D Detected, *ND* Not detected, *L1* Photolysis using L1 lamp, *L1/H_2O_2* Photo-H_2O_2 process using L1 lamp, *L2/F* Photo-Fenton process using L2 lamp, *F* Fenton process

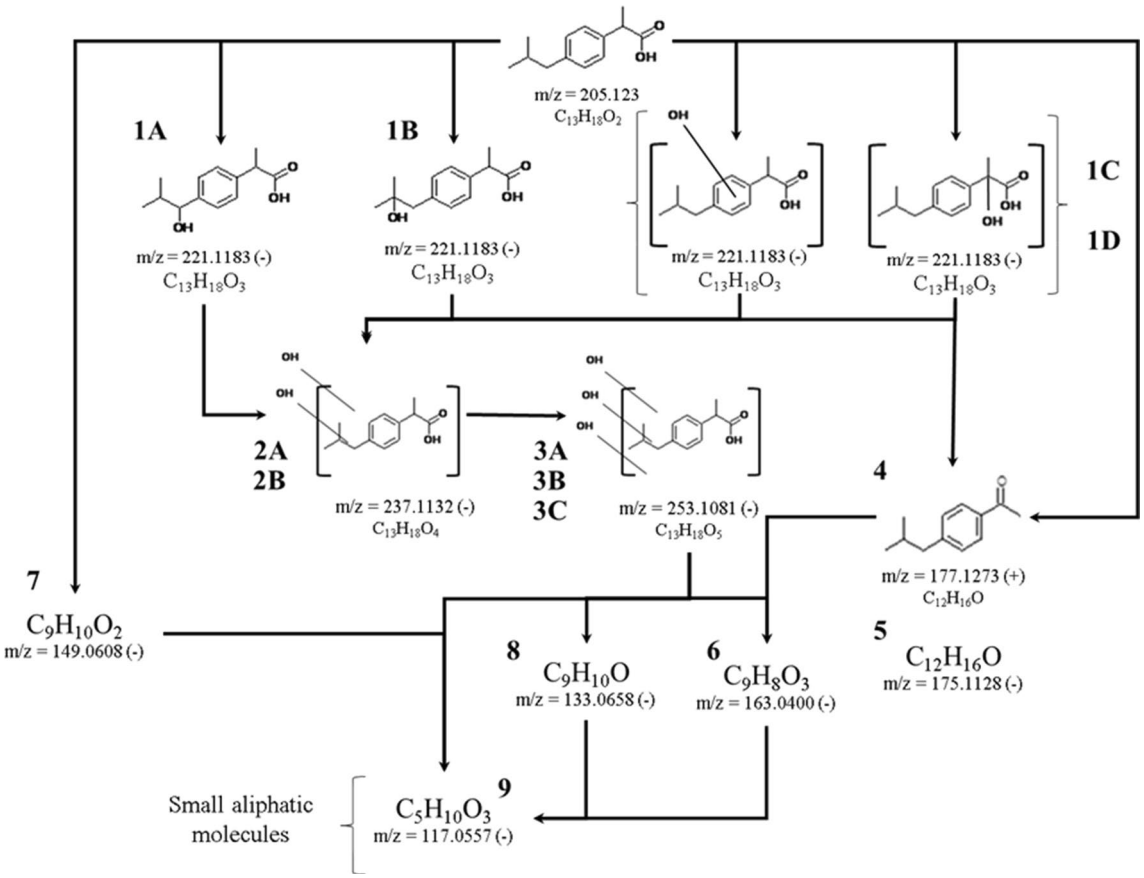

Fig. 6 Proposed IBP degradation scheme during photo-based AOPs

further hydroxylated, forming TP2 ($C_{13}H_{18}O_4$), then TP3 ($C_{13}H_{18}O_5$) isomers. In the investigated reactions, up to two di-hydroxylated and three tri-hydroxylated isomers were observed, but their structure could not be identified in detail with the mass spectrometer used.

Interestingly, only three hydroxylated transformation products (i.e., TP1C, TP1D, TP2B) were formed during photolysis (L1) compared with nine such products in the L1/H_2O_2 and L2/Fenton processes (i.e., TP1A-D, TP2A-B, and TP3A-C). This could be explained by either a lower mineralization efficiency or the contribution of non-radical mechanisms during photolysis (e.g., direct photo-degradation). The fact that 4-isobutylacetophenone (TP4)—a more toxic intermediate—was only found during photolysis is in line with the latter hypothesis. This compound can indeed be formed either by decarboxylation of hydroxylated IBP (Méndez-Arriaga et al. 2010; Michael et al. 2014) or by direct photo-decarboxylation of IBP (Jacobs et al. 2011; Ruggeri et al. 2013). Its constitutional isomer TP5 (Méndez-Arriaga et al. 2010), however, was detected in all cases. Successive hydroxylations and the loss of TP4's terminal propyl group can then lead to the formation of TP6 ($C_9H_8O_3$) and TP8 ($C_9H_{10}O$) (da Silva et al. 2014).

A parallel degradation pathway for IBP involves the cleavage of the isobutyl moiety, forming 2-phenyl-propionic acid ($C_9H_{10}O_2$, TP7) (Illés et al. 2013; Michael et al. 2014).

Finally, ring opening leads to the formation of small aliphatic molecules, such as TP9 ($C_5H_{10}O_3$), which was found in all the experiments.

The proposed IBP degradation scheme, based on the present results and information from previous studies, is shown in Fig. 6. Note that dark Fenton oxidation produced all the above-described species, except for 1- and 2-hydroxy-IBP and TP4.

Conclusion

This paper describes the degradation of IBP in several photo-based AOPs, with different types of lamp. For photolysis, the MP Hg lamp (L3) was found to be much more effective than the LP Hg lamps (L1 and L1′) and the xenon-arc lamp (L2). Adding H_2O_2 or Fenton reagent in moderate excess significantly enhanced both the IBP degradation rate and the TOC removal yield, reducing the electric energy demand (EEO criterion) by at least one order of magnitude in terms of pollutant conversion. Coupling ultrasound with the photo-Fenton process was only found to be beneficial at a low Fe/IBP molar ratio (~0.3), and to a limited extent. (The improvement in the mineralization yield was negligible.) High concentrations of oxidant (H_2O_2/IBP > 50) or of Fenton reagent were required to obtain high mineralization yields in all the processes. The different transformation products identified during photolysis and photo-oxidation (in the presence of H_2O_2 or Fenton reagent) highlighted the contributions of radical attack with successive hydroxylations, but a non-radical pathway was also identified during photolysis, in keeping with the direct photo-degradation of the molecule observed when methanol was added as a radical scavenger.

Supplementary Information The online version contains supplementary material available at https://doi.org/10.1007/s13762-021-03372-5.

Acknowledgements This study was supported by ANR (French National Research Agency) through ANR Project "SOFENcoMEM" (ANR-14-CE04-0006). Sandyanto Adityosulindro is grateful to the RISTEKDIKTI (Ministry of Research, Technology and Higher Education of Indonesia) for the award of a PhD scholarship (2017/E4.4/K/2013). Technical supports by M. L. Pern (LGC), G. Guittier (LGC), and J. L. Labat (LGC) are also gratefully acknowledged.

Declarations

Conflict of interest The authors declare that they have no conflict of interest.

References

Adak A, Das I, Mondal B et al (2019) Degradation of 2,4-dichlorophenoxyacetic acid by UV 253.7 and UV-H2O2: reaction kinetics and effects of interfering substances. Emerg Contam 5:53–60. https://doi.org/10.1016/j.emcon.2019.02.004

Adityosulindro S, Barthe L, González-Labrada K et al (2017) Sonolysis and sono-Fenton oxidation for removal of ibuprofen in (waste) water. Ultrason Sonochem 39:889–896. https://doi.org/10.1016/j.ultsonch.2017.06.008

Adityosulindro S, Julcour C, Barthe L (2018) Heterogeneous Fenton oxidation using Fe-ZSM5 catalyst for removal of ibuprofen in wastewater. J Environ Chem Eng 6:5920–5928. https://doi.org/10.1016/j.jece.2018.09.007

Andreozzi R (1999) Advanced oxidation processes (AOP) for water purification and recovery. Catal Today 53:51–59. https://doi.org/10.1016/S0920-5861(99)00102-9

Babuponnusami A, Muthukumar K (2014) A review on Fenton and improvements to the Fenton process for wastewater treatment. J Environ Chem Eng 2:557–572. https://doi.org/10.1016/j.jece.2013.10.011

Bagal MV, Gogate PR (2014) Wastewater treatment using hybrid treatment schemes based on cavitation and Fenton chemistry: a review. Ultrason Sonochem 21:1–14

Bolton JR, Bircher KG, Tumas W, Tolman CA (2001) Figures-of-merit for the technical development and application of advanced oxidation technologies for both electric- and solar-driven systems (IUPAC Technical Report). Pure Appl Chem 73:627–637

Burns EE, Carter LJ, Kolpin DW et al (2018) Temporal and spatial variation in pharmaceutical concentrations in an urban river system. Water Res 137:72–85. https://doi.org/10.1016/j.watres.2018.02.066

Cabrera Reina A, Miralles-Cuevas S, Cornejo L et al (2020) The influence of location on solar photo-Fenton: Process performance, photoreactor scaling-up and treatment cost. Renew Energy 145:1890–1900. https://doi.org/10.1016/j.renene.2019.07.113

Carlsson C, Johansson A-K, Alvan G et al (2006) Are pharmaceuticals potent environmental pollutants? Part I: environmental risk assessments of selected active pharmaceutical ingredients. Sci Total Environ 364:67–87. https://doi.org/10.1016/j.scitotenv.2005.06.035

Chakma S, Moholkar VS (2014) Investigations in synergism of hybrid advanced oxidation processes with combinations of sonolysis + Fenton process + UV for degradation of bisphenol A. Ind Eng Chem Res 53:6855–6865

Cruz González G, Julcour C, Chaumat H et al (2018) Degradation of 2,4-dichlorophenoxyacetic acid by photolysis and photo-Fenton oxidation. J Environ Chem Eng 6:874–882. https://doi.org/10.1016/j.jece.2017.12.049

da Silva JCC, Teodoro JAR, Afonso RJDCF et al (2014) Photolysis and photocatalysis of ibuprofen in aqueous medium: characterization of by-products via liquid chromatography coupled to high-resolution mass spectrometry and assessment of their toxicities against *Artemia salina*. J Mass Spectrom 49:145–153. https://doi.org/10.1002/jms.3320

Deblonde T, Cossu-Leguille C, Hartemann P (2011) Emerging pollutants in wastewater: a review of the literature. Int J Hyg Environ Health 214:442–448. https://doi.org/10.1016/j.ijheh.2011.08.002

Du J, Mei C-F, Ying G-G, Xu M-Y (2016) Toxicity thresholds for diclofenac, acetaminophen and ibuprofen in the water flea *Daphnia magna*. Bull Environ Contam Toxicol 97:84–90. https://doi.org/10.1007/s00128-016-1806-7

Dükkancı M, Vinatoru M, Mason TJ (2014) The sonochemical decolourisation of textile azo dye Orange II: effects of Fenton type reagents and UV light. Ultrason Sonochem 21:846–853

Fekadu S, Alemayehu E, Dewil R, Van der Bruggen B (2019) Pharmaceuticals in freshwater aquatic environments: a comparison of the African and European challenge. Sci Total Environ 654:324–337. https://doi.org/10.1016/j.scitotenv.2018.11.072

Foteinis S, Monteagudo JM, Durán A, Chatzisymeon E (2018) Environmental sustainability of the solar photo-Fenton process for wastewater treatment and pharmaceuticals mineralization at semi-industrial scale. Sci Total Environ 612:605–612. https://doi.org/10.1016/j.scitotenv.2017.08.277

Funai DH, Didier F, Giménez J et al (2017) Photo-Fenton treatment of valproate under UVC, UVA and simulated solar radiation. J Hazard Mater 323:537–549

Gadipelly C, Pérez-González A, Yadav GD et al (2014) Pharmaceutical industry wastewater: review of the technologies for water treatment and reuse. Ind Eng Chem Res 53:11571–11592. https://doi.org/10.1021/ie501210j

Gonzalez MG, Oliveros E, Wörner M, Braun AM (2004) Vacuum-ultraviolet photolysis of aqueous reaction systems. J Photochem Photobiol C Photochem Rev 5:225–246. https://doi.org/10.1016/j.jphotochemrev.2004.10.002

Gonzalez-Olmos R, Holzer F, Kopinke F-D, Georgi A (2011) Indications of the reactive species in a heterogeneous Fenton-like reaction using Fe-containing zeolites. Appl Catal A Gen 398:44–53. https://doi.org/10.1016/j.apcata.2011.03.005

Gonzalez-Olmos R, Martin MJ, Georgi A et al (2012) Fe-zeolites as heterogeneous catalysts in solar Fenton-like reactions at neutral pH. Appl Catal B Environ 125:51–58. https://doi.org/10.1016/j.apcatb.2012.05.022

He J, Yang X, Men B, Wang D (2016) Interfacial mechanisms of heterogeneous Fenton reactions catalyzed by iron-based materials: a review. J Environ Sci. https://doi.org/10.1016/j.jes.2015.12.003

Illés E, Takács E, Dombi A et al (2013) Hydroxyl radical induced degradation of ibuprofen. Sci Total Environ 447:286–292. https://doi.org/10.1016/j.scitotenv.2013.01.007

Jacobs LE, Fimmen RL, Chin Y-P et al (2011) Fulvic acid mediated photolysis of ibuprofen in water. Water Res 45:4449–4458. https://doi.org/10.1016/j.watres.2011.05.041

Jakimska A, Śliwka-Kaszyńska M, Reszczyńska J et al (2014) Elucidation of transformation pathway of ketoprofen, ibuprofen, and furosemide in surface water and their occurrence in the aqueous environment using UHPLC-QTOF-MS. Anal Bioanal Chem 406:3667–3680. https://doi.org/10.1007/s00216-014-7614-1

Jallouli N, Pastrana-Martínez LM, Ribeiro AR et al (2018) Heterogeneous photocatalytic degradation of ibuprofen in ultrapure water, municipal and pharmaceutical industry wastewaters using a TiO_2/UV-LED system. Chem Eng J 334:976–984. https://doi.org/10.1016/j.cej.2017.10.045

Klavarioti M, Mantzavinos D, Kassinos D (2009) Removal of residual pharmaceuticals from aqueous systems by advanced oxidation processes. Environ Int 35:402–417. https://doi.org/10.1016/j.envint.2008.07.009

Kwon M, Kim S, Yoon Y et al (2015) Comparative evaluation of ibuprofen removal by UV/H_2O_2 and UV/$S_2O_8^{2-}$ processes for wastewater treatment. Chem Eng J 269:379–390. https://doi.org/10.1016/j.cej.2015.01.125

Li FH, Yao K, Lv WY et al (2015) Photodegradation of ibuprofen under UV–Vis irradiation: mechanism and toxicity of photolysis products. Bull Environ Contam Toxicol 94:479–483. https://doi.org/10.1007/s00128-015-1494-8

Li Y, Zhang L, Liu X, Ding J (2019) Ranking and prioritizing pharmaceuticals in the aquatic environment of China. Sci Total Environ 658:333–342. https://doi.org/10.1016/j.scitotenv.2018.12.048

Lindim C, de Zwart D, Cousins IT et al (2019) Exposure and ecotoxicological risk assessment of mixtures of top prescribed pharmaceuticals in Swedish freshwaters. Chemosphere 220:344–352. https://doi.org/10.1016/j.chemosphere.2018.12.118

Loaiza-Ambuludi S, Panizza M, Oturan N, Oturan MA (2014) Removal of the anti-inflammatory drug ibuprofen from water using homogeneous photocatalysis. Catal Today 224:29–33. https://doi.org/10.1016/j.cattod.2013.12.018

Madhavan J, Grieser F, Ashokkumar M (2010a) Combined advanced oxidation processes for the synergistic degradation of ibuprofen in aqueous environments. J Hazard Mater 178:202–208

Madhavan J, Sathish Kumar PS, Anandan S et al (2010b) Sonophotocatalytic degradation of monocrotopos usingh TiO_2 and Fe^{3+}. J Hazard Mater 177:944–949. https://doi.org/10.1016/j.jhazmat.2010.01.009

Madhavan J, Sathish Kumar PS, Anandan S et al (2010c) Degradation of acid red 88 by the combination of sonolysis and photocatalysis. Sep Purif Technol 74:336–341. https://doi.org/10.1016/j.seppur.2010.07.001

Madhavan J, Grieser F, Ashokkumar M (2013) Sonophotocatalytic degradation of paracetamol using TiO_2 and Fe^{3+}. Sep Purif Technol 103:114–118. https://doi.org/10.1016/j.seppur.2012.10.003

Méndez-Arriaga F, Torres-Palma RA, Pétrier C et al (2009) Mineralization enhancement of a recalcitrant pharmaceutical pollutant in water by advanced oxidation hybrid processes. Water Res 43:3984–3991

Méndez-Arriaga F, Esplugas S, Giménez J (2010) Degradation of the emerging contaminant ibuprofen in water by photo-Fenton. Water Res 44:589–595

Michael I, Achilleos A, Lambropoulou D et al (2014) Proposed transformation pathway and evolution profile of diclofenac and ibuprofen transformation products during (sono)photocatalysis. Appl Catal B Environ 147:1015–1027

Miklos DB, Remy C, Jekel M et al (2018) Evaluation of advanced oxidation processes for water and wastewater treatment—a critical review. Water Res 139:118–131. https://doi.org/10.1016/j.watres.2018.03.042

Miralles-Cuevas S, Arqués A, Maldonado MI et al (2013) Combined nanofiltration and photo-Fenton treatment of water containing micropollutants. Chem Eng J 224:89–95. https://doi.org/10.1016/j.cej.2012.09.068

Mirzaei A, Chen Z, Haghighat F, Yerushalmi L (2017) Removal of pharmaceuticals from water by homo/heterogonous Fenton-type processes—a review. Chemosphere 174:665–688. https://doi.org/10.1016/j.chemosphere.2017.02.019

Mrowetz M, Pirola C, Selli E (2003) Degradation of organic water pollutants through sonophotocatalysis in the presence of TiO(2). Ultrason Sonochem 10:247–254. https://doi.org/10.1016/S1350-4177(03)00090-7

Munter R (2001) Advanced oxidation processes-current status and prospects. Proc Est Acad Sci Chem 50:59–80

Na S, Jinhua C, Cui M, Khim J (2012) Sonophotolytic diethyl phthalate (DEP) degradation with UVC or VUV irradiation. Ultrason Sonochem 19:1094–1098

Nichela DA, Donadelli JA, Caram BF et al (2015) Iron cycling during the autocatalytic decomposition of benzoic acid derivatives by Fenton-like and photo-Fenton techniques. Appl Catal B Environ 170–171:312–321. https://doi.org/10.1016/j.apcatb.2015.01.028

O'Sullivan DW, Tyree M (2007) The kinetics of complex formation between Ti(IV) and hydrogen peroxide. Int J Chem Kinet 39:457–461

Oppenländer T (2003) Photochemical purification of water and air, advanced oxidation processes: principles, reaction mechanisms, reactor concepts. Wiley-VCH, Weinheim

Packer JL, Werner JJ, Latch DE et al (2003) Photochemical fate of pharmaceuticals in the environment: naproxen, diclofenac, clofibric acid, and ibuprofen. Aquat Sci 65:342–351. https://doi.org/10.1007/s00027-003-0671-8

Papoutsakis S, Miralles-Cuevas S, Gondrexon N et al (2015) Coupling between high-frequency ultrasound and solar photo-Fenton at pilot scale for the treatment of organic contaminants: an initial approach. Ultrason Sonochem 22:527–534. https://doi.org/10.1016/j.ultsonch.2014.05.003

Parolini M (2020) Toxicity of the non-steroidal anti-inflammatory drugs (NSAIDs) acetylsalicylic acid, paracetamol, diclofenac, ibuprofen and naproxen towards freshwater invertebrates: a review. Sci Total Environ 740:140043. https://doi.org/10.1016/j.scitotenv.2020.140043

Parsons S (2004) Advanced oxidation processes for water and wastewater treatment. IWA Publishing, London

Pérez M (2002) Fenton and photo-Fenton oxidation of textile effluents. Water Res 36:2703–2710. https://doi.org/10.1016/S0043-1354(01)00506-1

Petrie B, Barden R, Kasprzyk-Hordern B (2015) A review on emerging contaminants in wastewaters and the environment: current knowledge, understudied areas and recommendations for future monitoring. Water Res 72:3–27. https://doi.org/10.1016/j.watres.2014.08.053

Quero-Pastor MJ, Garrido-Perez MC, Acevedo A, Quiroga JM (2014) Ozonation of ibuprofen: a degradation and toxicity study. Sci Total Environ 466–467:957–964. https://doi.org/10.1016/j.scitotenv.2013.07.067

Rehman MSU, Rashid N, Ashfaq M et al (2015) Global risk of pharmaceutical contamination from highly populated developing countries. Chemosphere 138:1045–1055. https://doi.org/10.1016/j.chemosphere.2013.02.036

Rodríguez EM, Núñez B, Fernández G, Beltrán FJ (2009) Effects of some carboxylic acids on the Fe(III)/UVA photocatalytic oxidation of muconic acid in water. Appl Catal B Environ 89:214–222. https://doi.org/10.1016/j.apcatb.2008.11.030

Rosman N, Salleh WNW, Mohamed MA et al (2018) Hybrid membrane filtration-advanced oxidation processes for removal of pharmaceutical residue. J Colloid Interface Sci 532:236–260. https://doi.org/10.1016/j.jcis.2018.07.118

Ruggeri G, Ghigo G, Maurino V et al (2013) Photochemical transformation of ibuprofen into harmful 4-isobutylacetophenone: pathways, kinetics, and significance for surface waters. Water Res 47:6109–6121. https://doi.org/10.1016/j.watres.2013.07.031

Safarzadeh-Amiri A, Bolton JR, Cater SR (1997) Ferrioxalate-mediated photodegradation of organic pollutants in contaminated water. Water Res 31:787–798. https://doi.org/10.1016/S0043-1354(96)00373-9

Shahbazi A, Gonzalez-Olmos R, Kopinke F-D et al (2014) Natural and synthetic zeolites in adsorption/oxidation processes to remove surfactant molecules from water. Sep Purif Technol 127:1–9. https://doi.org/10.1016/j.seppur.2014.02.021

Shu Z, Bolton JR, Belosevic M, El Din MG (2013) Photodegradation of emerging micropollutants using the medium-pressure UV/H_2O_2 advanced oxidation process. Water Res 47:2881–2889. https://doi.org/10.1016/j.watres.2013.02.045

Son H-S, Im J-K, Zoh K-D (2009) A Fenton-like degradation mechanism for 1,4-dioxane using zero-valent iron (Fe^0) and UV light. Water Res 43:1457–1463. https://doi.org/10.1016/j.watres.2008.12.029

Sophia AC, Lima EC (2018) Removal of emerging contaminants from the environment by adsorption. Ecotoxicol Environ Saf 150:1–17. https://doi.org/10.1016/j.ecoenv.2017.12.026

Syakti AD, Ahmed MM, Hidayati NV et al (2013) Screening of emerging pollutants in the mangrove of Segara Anakan Nature Reserve, Indonesia. IERI Procedia 5:216–222. https://doi.org/10.1016/j.ieri.2013.11.095

Szabó RK, Megyeri C, Illés E et al (2011) Phototransformation of ibuprofen and ketoprofen in aqueous solutions. Chemosphere 84:1658–1663. https://doi.org/10.1016/j.chemosphere.2011.05.012

Tayo L, Caparanga A, Doma B, Liao C-H (2018) A review on the removal of pharmaceutical and personal care products (PPCPs) using advanced oxidation processes. J Adv Oxid Technol. https://doi.org/10.26802/jaots.2017.0079

Tiwari B, Sellamuthu B, Ouarda Y et al (2017) Review on fate and mechanism of removal of pharmaceutical pollutants from wastewater using biological approach. Bioresour Technol 224:1–12. https://doi.org/10.1016/j.biortech.2016.11.042

Tokumura M, Sugawara A, Raknuzzaman M et al (2016) Comprehensive study on effects of water matrices on removal of pharmaceuticals by three different kinds of advanced oxidation processes. Chemosphere 159:317–325. https://doi.org/10.1016/j.chemosphere.2016.06.019

Torres RA, Sarantakos G, Combet E et al (2008) Sequential helio-photo-Fenton and sonication processes for the treatment of bisphenol A. J Photochem Photobiol A Chem 199:197–203

Velichkova F, Delmas H, Julcour C, Koumanova B (2016) Heterogeneous Fenton and photo-Fenton oxidation for paracetamol removal using iron containing ZSM-5 zeolite as catalyst. AIChE J 63:669–679. https://doi.org/10.1002/aic.15369

Välitalo P, Kruglova A, Mikola A, Vahala R (2017) Toxicological impacts of antibiotics on aquatic micro-organisms: a mini-review. Int J Hyg Environ Health 220:558–569. https://doi.org/10.1016/j.ijheh.2017.02.003

Waite TD, Morel FMM (1984) Photoreductive dissolution of colloidal iron oxides in natural waters. Environ Sci Technol 18:860–868. https://doi.org/10.1021/es00129a010

Wang X-H, Lin AY-C (2014) Is the phototransformation of pharmaceuticals a natural purification process that decreases ecological and human health risks? Environ Pollut 186:203–215. https://doi.org/10.1016/j.envpol.2013.12.007

Wang L, Peng Y, Nie X et al (2016) Gene response of CYP360A, CYP314, and GST and whole-organism changes in *Daphnia magna* exposed to ibuprofen. Comp Biochem Physiol Part C Toxicol Pharmacol 179:49–56. https://doi.org/10.1016/j.cbpc.2015.08.010

Weavers LK, Ling FH, Hoffmann MR (1998) Aromatic compound degradation in water using a combination of sonolysis and ozonolysis. Environ Sci Technol 32:2727–2733. https://doi.org/10.1021/es970675a

Wols BA, Hofman-Caris CHM (2012) Review of photochemical reaction constants of organic micropollutants required for UV advanced oxidation processes in water. Water Res 46:2815–2827. https://doi.org/10.1016/j.watres.2012.03.036

Xu X-R, Li X-Y, Li X-Z, Li H-B (2009) Degradation of melatonin by UV, UV/H_2O_2, Fe^{2+}/H_2O_2 and UV/Fe^{2+}/H_2O_2 processes. Sep Purif Technol 68:261–266. https://doi.org/10.1016/j.seppur.2009.05.013

Xu LJ, Chu W, Graham N (2013) Degradation of di-n-butyl phthalate by a homogeneous sono-photo-Fenton process with in-situ generated hydrogen peroxide. Chem Eng J 240:541–547

Zhang M, Dong H, Zhao L et al (2019) A review on Fenton process for organic wastewater treatment based on optimization perspective. Sci Total Environ 670:110–121. https://doi.org/10.1016/j.scitotenv.2019.03.180

Zwiener C (2000) Oxidative treatment of pharmaceuticals in water. Water Res 34:1881–1885. https://doi.org/10.1016/S0043-1354(99)00338-3